Ultrafast Dynamics in the Three-Photon, Double-Resonance Ionization of Phenol via the S_2 Electronic State

Carolyn P. Schick and Peter M. Weber*

Department of Chemistry, Brown University, Providence, Rhode Island 02912

Received: September 16, 2000; In Final Form: January 23, 2001

The three-photon ionization pathways of phenol involving the S_2 electronic state as well as higher molecular resonances are explored. Photoelectron spectra are obtained upon ionization with femtosecond laser pulses at 206 and 412 nm. In addition to the well-known two-photon ionization signal, there is a small component in the spectrum that stems from a three-photon pathway. This path is resonant with the both the S_2 state and a superexcited state at 9 eV. The dependence of the three-photon pathway on the laser polarization suggests that the optically bright superexcited state has the same symmetry as the S_2 state. Upon two-photon excitation of the superexcited state, a nonradiative decay leads to the population of a set of Rydberg states, which can be ionized by a third laser photon. Photoelectron spectra taken with a time delay between the fourth-harmonic pulse, which prepares the molecule in the S_2 state, and the second-harmonic pulse, which ionizes the molecule via the superexcited states, reflect the internal conversion dynamics of S_2 to S_1. We also observe a component of the three-photon ionization signal that persists beyond the decay time of the S_2 state, which suggests that a separate ionization path becomes accessible after the internal conversion to S_1. This path may involve another recently discovered valence state with an energy of 7.5 eV. The effect of this latter ionization pathway on the interpretation of time-resolved multiphoton ionization experiments is discussed.

Introduction

Highly excited states of molecules are fascinating from a fundamental perspective and important for many contemporary problems in chemistry. When excited beyond the first absorption band, molecules exhibit a rich photophysics, including internal conversion to lower electronic states of the same spin multiplicity, intersystem crossing to electronic states with different spins, and radiative emission to lower surfaces. In addition, since the excitation energies often exceed those of a typical chemical bond, there are photochemical reactions such as isomerization, fragmentation, or, in the case of cyclic molecules, ring-opening reactions. These photochemical reactions have practical applications in synthetic chemistry and medical applications in phototherapy. They are also featured prominently in radiation chemistry and the photochemistry of the upper atmosphere. Moreover, excited states of molecules play a role in chemical instrumentation, such as the fragmentation of molecules in mass spectrometers. Finally, many experiments exploring the reaction mechanisms of excited molecules using ultrafast spectroscopies involve electronically excited states. The behavior of molecules in highly excited electronic states is therefore a cornerstone of modern chemistry.

We use multiphoton ionization photoelectron spectroscopy with short laser pulses as a tool to map the pathways of energy flow in molecules. Time-resolved multiphoton ionization photoelectron spectroscopy experiments have recently become very popular because they produce a tremendous amount of information about molecular relaxation phenomena. Examples of such studies include the observation of intersystem crossing in benzene[1] and vibrational relaxation in alkylanilines[2] by the Reilly group, intersystem crossing from S_1 to T_1 in pyrazine by the Johnson group,[3,4] studies of electronic and vibrational relaxation in benzene and fluorene by the Knee group,[5] femtosecond time-resolved studies of internal conversion in linear hexatriene chains by Hayden, Chandler, and co-workers,[6,7] femtosecond studies of internal conversion in benzene and benzene dimers by Radloff et al.,[8] wave packet and electronic relaxation studies in iodine and other molecules by Stolow and co-workers,[9,10] and time-resolved studies of the ultrafast dynamics in small molecular clusters by the Neumark group.[11−14] In our own laboratory, we have investigated the electronic relaxation in azulene,[15] phenanthrene,[16,17] aniline and aminopyridine,[18−20] and phenol.[21] All of these studies rely on the ionization of molecules by sequences of short laser pulses. The nonradiative processes are reflected in the photoelectron spectra by a change in the kinetic energy of the ejected electrons. It is the aim of this paper to revisit some of the assumptions that are made in the analysis of those photoelectron spectra in light of our recent discovery of superexcited states, which provide additional pathways to photoionization.[22]

While studying the photoionization dynamics of phenol via the S_1 electronic state, we discovered a small amount of signal that originates from a three-photon ionization process. As was described in detail,[22] this photoionization results in a richly structured photoelectron spectrum stretching from 8.5 to 12 eV. We found that the spectrum can arise from two distinct double-resonance ionization schemes. In one scheme, the first photon is resonant with the S_1 electronic state, and the second photon is resonant with an optically bright superexcited state at 9 eV. The superexcited state contains admixtures of a doubly excited valence state with an electron configuration of $...(16)^2(17)^2(18)^0(19)^2$. This valence state features a very short lifetime. Decay channels include autoionization, as well as a nonradiative decay to a set of Rydberg levels. From those Rydberg levels, a third 3ω photon, or a time-delayed second-harmonic (2ω) photon, can ionize the molecule. The observed

10.1021/jp003304g CCC: $20.00
Published on Web 03/21/2001

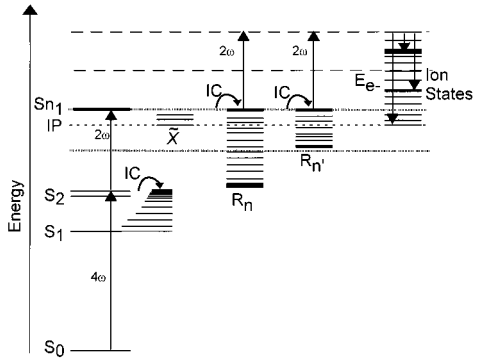

Figure 1. Three-photon ionization of phenol via the S_2 electronic state. A fourth-harmonic (4ω) photon lifts the molecule to S_2, and a second-harmonic photon (2ω) excites it to superexcited states at 9 eV. Ultrafast internal conversion (IC) from this state populates a set of Rydberg levels, R_n, which are then ionized by a third photon. The ionization energy (IP) is 8.51 eV.

electronic states can be assigned to Rydberg series with constant quantum defect.

The other ionization path involves a singly excited valence state around 7.5 eV, below the ionization energy of phenol. To access this state, the molecule is prepared in the S_1 state by the absorption of a 3ω photon. Then, a 2ω photon promotes an electron from orbital 16 to orbital 18, resulting in a state with a nominal electron configuration of $...(16)^1(17)^2(18)^2(19)^1$. This state decays to the energetically accessible subset of Rydberg levels. Ionization then proceeds out of these Rydberg levels, producing a photoelectron spectrum very similar to the one following the path via the 9 eV resonance. The restriction imposed by the lower resonance energy leads, however, to a characteristic onset that appears in the photoelectron spectrum at 10 eV.

The specific question that we address in this paper is how these highly excited valence states affect the photoelectron spectra of phenol taken via the S_2 electronic state. In a recent paper, we have studied the internal conversion of S_2 to S_1 in phenol by time-resolved two-photon ionization.[21] A fourth-harmonic (4ω) laser pulse around 210 nm prepares the molecule in S_2, and a second-harmonic (2ω) laser pulse around 420 nm ionizes the molecule. Measurement of the photoelectron spectra as a function of the time delay between the 4ω and the 2ω pulses maps the decay of the S_2 state. In the spectra we noted a significant background signal with a distinct time dependence, which might affect the measured time scale of the internal conversion dynamics. Indeed, Stolow and co-workers suggest that the internal conversion from S_2 to S_1 might proceed on a time scale as fast as 50 fs.[23] Further studies of the photoelectron spectra of phenol with 4ω and 2ω photons now suggest that, underlying the two-photon ionization photoelectron signals, there are three-photon processes that generate a background with a distinct time evolution.

Our experiments are described using the scheme shown in Figure 1. The fourth-harmonic photon, 4ω, is resonant with the $S_0 \rightarrow S_2$ transition. The three-photon ionization pathway features a further excitation to the superexcited state, S_{n1}, at 9 eV, which rapidly relaxes into a set of Rydberg states. Only two states, R_n and $R_{n'}$, are shown in the illustration. Ionization proceeds with a third photon. Since the potential energy surfaces of the Rydberg states closely resemble those of the ion, the ionization preserves the vibrational energy content of the molecule. Sharp lines are therefore observed, one for each Rydberg state.

The availability of a three-photon ionization pathway in the $4\omega + 2\omega + 2\omega$ scheme allows us to explore a set of questions that complement those that we pursued using the $3\omega + 3\omega + 3\omega$ scheme.[22] Specifically, we gain further insights into the electronic makeup of the superexcited state at 9 eV, and information about the symmetry of the superexcited state by studying the dependence of the $4\omega + 2\omega + 2\omega$ signal on the relative polarizations of the 4ω and 2ω photons. The dependence of the $4\omega + 2\omega + 2\omega$ photoelectron spectra on the time delay between the 4ω and the 2ω photons is measured. This delay maps the dynamics of the internal conversion from S_2 to S_1, similar to the two-photon ionization process. Surprisingly, we observe a dramatically different time dependence in the three-photon process compared to the two-photon process. This time dependence sheds further light on the different ionization pathways available to the molecule via highly excited resonances. It also allows us to discuss the implications that superexcited states may have on the observation and analysis of time-resolved multiphoton ionization and photoelectron experiments.

Experimental Section

The details of the experimental apparatus have been described in significant detail before.[19−22,24] We generate the second and fourth harmonics (412 and 206 nm) from a regeneratively amplified titanium:sapphire laser system with a 50 kHz repetition rate. The two-photon ionization with 4ω and 2ω photons results in a clean ionization with almost no fragmentation. The mass spectrum, which has been reproduced elsewhere,[25] shows only the parent ion prominently. In the $4\omega + 2\omega$ ionization scheme, there is a very small amount of fragmentation (2.4% total), even less than observed in the ionization with third-harmonic pulses. The fragments that we observe are typical for phenol. There is no indication of impurities.

Results and Discussion

$4\omega + 2\omega + 2\omega$ Spectrum. The ionization of phenol with only fourth-harmonic laser pulses (206 nm) leads to two-photon ionization photoelectron spectra showing prominently the ground electronic state of the ion. When phenol is irradiated with second-harmonic laser pulses (412 nm) only, there is a weak, but measurable signal. Consistent with an ionization energy of 8.51 eV,[26,27] most of this signal arises from three-photon ionization. There is also a very small amount of signal stemming from a four-photon ionization. That spectrum has been presented and discussed previously.[22]

Ionization with both the fourth-harmonic and the second-harmonic laser pulses, overlapped in space and time, leads to additional ionization pathways. The dominant path is $4\omega + 2\omega$, in which a fourth-harmonic photon excites the molecule to S_2 and a second-harmonic photon ionizes the molecule. The electron signal, which can be used to measure the decay of the S_2 state, has also been described previously.[21] In addition, we observe a small amount of fast photoelectrons, with energies up to 3.5 eV, which are generated in a $4\omega + 2\omega + 2\omega$ ionization mechanism. Since the total energy of one fourth-harmonic photon plus two second-harmonic photons just equals the energy of two fourth-harmonic photons, the signal from the three-photon processes partially overlaps that of the $4\omega + 4\omega$ process. To extract the signal stemming from the $4\omega + 2\omega + 2\omega$ ionization, we subtract a spectrum taken with only the 4ω photons present. This procedure has the systematic problem that it neglects the depletion of the $4\omega + 4\omega$ signal by the simultaneous presence of the 2ω photons. As a result, the spectra have considerable uncertainty in their overall intensity, especially in the range of 8.5−9.0 eV where the $4\omega + 4\omega$ signal is strongest. The higher

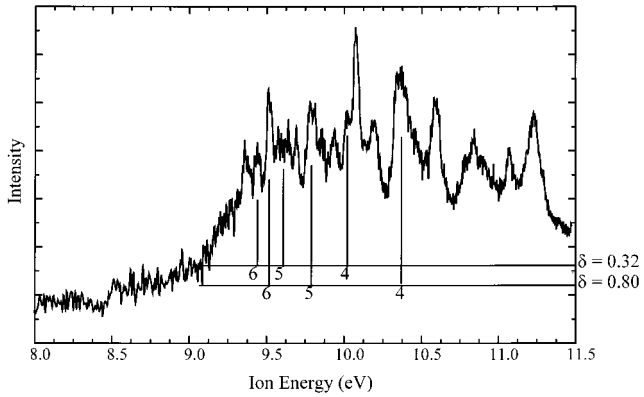

Figure 2. Photoelectron spectrum obtained with the $4\omega + 2\omega + 2\omega$ ionization scheme. Laser wavelengths: 206.2 nm (4ω), 412.5 nm (2ω). The Rydberg series are assigned as in ref 22 and are labeled with the reported n and δ values for this two-color ionization.

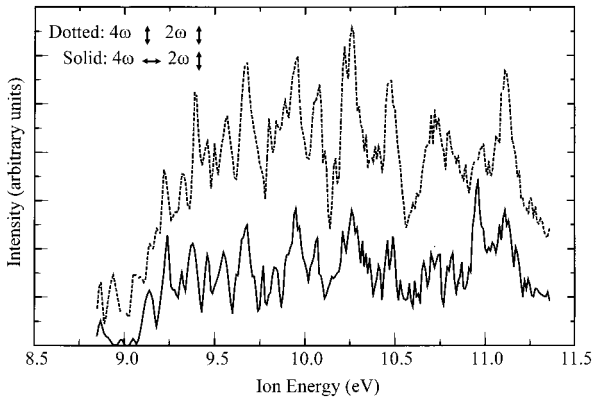

Figure 3. Effect of the polarization of the 4ω pulse on a $4\omega + 2\omega + 2\omega$ photoelectron spectrum. Dotted line: both 4ω and 2ω vertical (parallel to the detector direction). Solid line: 4ω horizontal and 2ω vertical. Laser wavelengths: 208.5 nm (4ω), 418.2 nm (2ω).

energy range, above 9 eV, is less affected by the $4\omega + 4\omega$ background, as the two-photon signal is significantly weaker in that range. The dominant part of the $4\omega + 2\omega + 2\omega$ spectrum, which stretches from about 9.4 to 11.4 eV, is therefore only slightly affected by the $4\omega + 4\omega$ background.

The $4\omega + 2\omega + 2\omega$ spectrum, shown in Figure 2, features a series of sharp peaks. All the peak positions and intensities closely correlate with those seen in the spectra obtained with $3\omega + 3\omega + 3\omega$, $3\omega + 3\omega + 2\omega$, and $2\omega + 2\omega + 2\omega + 2\omega$ ionization.[22] In accordance with our discussion of the $3\omega + 3\omega + 2\omega$ photoionization spectra, we interpret the peaks between 9.4 and 11.4 eV in the $4\omega + 2\omega + 2\omega$ spectrum as arising from Rydberg states that form series with various quantum defects. The assignment coincides with the one derived for the previous spectra. Two Rydberg series with quantum defects of 0.32 and 0.80 are indicated in Figure 2.

The spectrum in Figure 2 is taken with a 4ω wavelength of 206.2 nm and a 2ω wavelength of 412.5 nm. The two-photon resonance is therefore excited at an energy of 9.02 eV. We also obtained photoelectron spectra with longer 4ω and 2ω wavelengths, for example, 208 and 416 nm. The two-photon excitation energy is then 8.88 eV, which is 0.14 eV lower. The resulting spectrum is shifted by exactly the difference in the two-photon excitation energies. This supports our interpretation of the spectra as Rydberg states that are populated by an ultrafast conversion from a primary superexcited state. It is inconsistent with an interpretation of those peaks as electronic states of the ion other than $\tilde{X}$, or some progression in specific ion vibrations.

Polarization Dependence. The excitation of the primary superexcited state with two separate laser pulses in the $4\omega + 2\omega + 2\omega$ ionization experiment allows us to vary the respective polarizations of the photons. Two of the resulting spectra, taken at zero delay time, are shown in Figure 3. In both spectra, the excitation from S_2 to the primary superexcited state, as well as the ionization, proceeds with a vertically polarized 2ω photon. This polarization is parallel to the direction of the time-of-flight detector. The difference between the two spectra arises from the polarization of the 4ω photons. The dotted curve is the spectrum with a polarization of the 4ω photon parallel to that of the 2ω photon. The solid curve is for the two colors at perpendicular polarizations. It is evident that a parallel alignment of the 4ω and the 2ω polarizations leads to a significantly larger three-photon signal than a perpendicular alignment. One exception might be the peak at 11 eV. This curious peak also distinguishes itself by its time dependence.[22] At the present time, we have no explanation for its odd behavior.

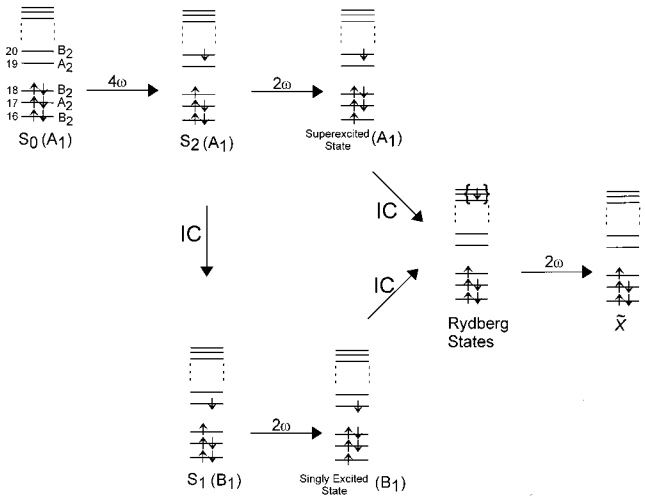

Figure 4. Doubly resonant, three-photon ionization pathways of phenol, using 4ω and 2ω pulses, illustrated by correlation diagrams.

The dependence of the photoelectron spectra on the laser polarization points to the orbitals that might be involved in the three-photon ionization process. The excitation from S_0 to S_2 promotes one electron from orbital 18 to orbital 20.[21] Both of these orbitals have B_2 symmetry, within the approximate C_{2v} point group of phenol. Thus, the S_2 electronic state has A_1 symmetry, and the transition $S_0 \rightarrow S_2$ is allowed with a transition dipole moment parallel to the molecular axis. The optical excitation therefore selects, out of the randomly oriented sample of molecules in the molecular beam, those molecules whose axis is preferentially aligned parallel to the polarization of the 4ω photons. Since the photoelectron spectra show that a parallel alignment of the 4ω and 2ω polarizations leads to a larger signal, we conclude that the transition dipole moment from the S_2 state to the primary superexcited state is parallel to the molecular axis as well. Thus, the primary superexcited state must have A_1 symmetry. Of course, we cannot rule out the existence of more than one superexcited state at 9 eV. Our experiment suggests, however, that the superexcited state responsible for most of the three-photon ionization signal has A_1 symmetry.

Figure 4 illustrates the three-photon ionization process using schematic correlation diagrams. The $S_0 \rightarrow S_2$ transition promotes an electron from orbital 18 to orbital 20. From there, the second photon excites a superexcited molecular state with A_1 symmetry. Note that this second step must involve electrons from other orbitals, since further excitation of the electron residing in orbital 20 with a 3 eV photon would eject it from the molecule.

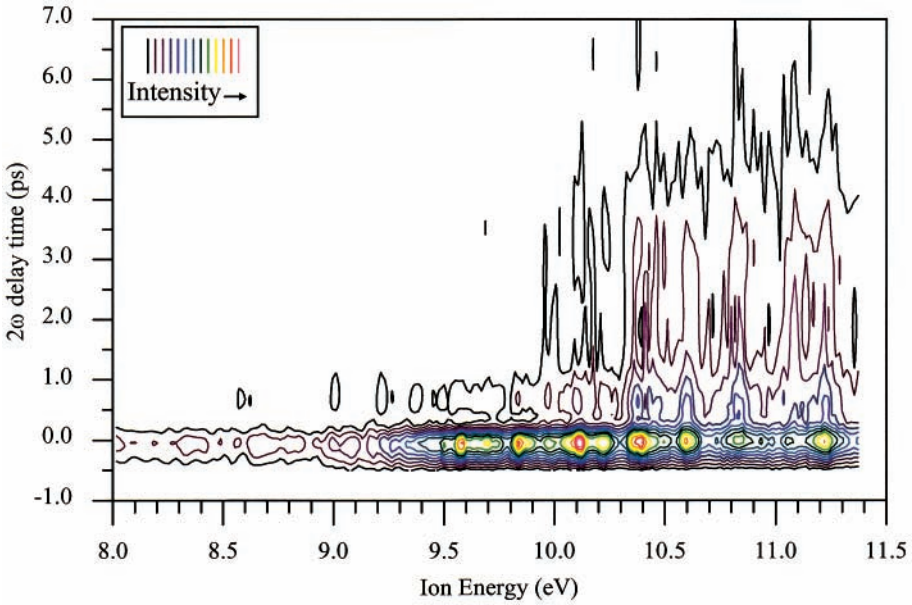

Figure 5. A contour plot showing the dependence of the $4\omega + 2\omega + 2\omega$ photoelectron signal on the delay time between the 4ω pulse and the 2ω pulse. Laser wavelengths: 206.6 nm (4ω), 413.7 nm (2ω).

There are several conceivable ways to promote another electron while maintaining A_1 symmetry. For example, a second electron from orbital 18 could be promoted to orbital 20. This transition would involve the same orbitals as the $S_0 \rightarrow S_2$ transition, and therefore should require about 6 eV of energy. Our second-harmonic photon with 3 eV of energy is not likely to induce this process. Next, an electron could be promoted from orbital 17 to orbital 19. However, since the HOMO−LUMO ($18 \rightarrow 19$) gap is known to be at 4.5 eV for both the neutral molecule[28] and the phenol ion,[29] this transition would most certainly require more than 3 eV. We thus exclude this scenario as well. A particularly attractive choice, however, is shown in Figure 4 (upper pathway). In this scheme, the second photon promotes an electron from orbital 16 to orbital 18. The energy gap between these two orbitals is known from photoelectron spectroscopy. The $\tilde{B}$ state of the ion is known to be 11.59 eV (vertical) above the ground state of the molecule,[29] or 3.1 eV above the ground state of the ion. This energy gap coincides with the 3 eV energy of the 2ω photon. Further evidence for a transition between orbitals 16 and 18 is seen in the absorption spectrum of the phenol ion. Kesper et al. observe a strong absorption band at 3 eV, exactly where one would expect the $16 \rightarrow 18$ transition to occur.[29] Thus, the most likely absorption of a 3 eV photon from the S_2 electronic state involves the excitation of an electron from orbital 16 to orbital 18. This suggests that the component of the primary superexcited state that provides the oscillator strength from S_2 has an electron configuration of $...(16)^1(17)^2(18)^2(19)^0(20)^1$.

We have previously discussed that the three-photon spectra via the S_1 electronic state were best explained by invoking a superexcited state that obtains its oscillator strength, as seen from S_1, on account of the electron configuration $...(16)^2(17)^2(18)^0(19)^2$.[22] The ionization via S_2 presented here suggests a different electron configuration, namely, $...(16)^1(17)^2(18)^2(19)^0(20)^1$. This should not be understood as a suggestion that there are two separate superexcited states with the same A_1 symmetry at 9 eV. Rather, we propose that there is a highly mixed valence state above the ionization energy that contains admixtures of both configurations. The different configurations provide oscillator strength from either S_1 or S_2.

The superexcited state is very short lived. As explained in our previous paper, ultrafast internal conversion leads to a set of Rydberg states, indicated by the Rydberg electron in braces in Figure 4, from which ionization proceeds by the absorption of another photon.

Time-Dependent Spectra. One of our objectives in this paper is to address how the existence of superexcited molecular states affects the measurement of ultrafast electronic relaxation in time-delayed ionization experiments. The superexcited states provide resonant ionization pathways that can compete with direct ionization, especially when high-power laser pulses are employed. At zero time delay, the three-photon signals are weak compared to the two-photon signals. However, at longer delays, when the two-photon signals decay due to electronic relaxation processes, the three-photon signals may, in fact, dominate the spectrum. We therefore investigated the dependence of the three-photon ionization signal on the delay time between the 4ω pulse that prepares the molecule in S_2 and the 2ω pulse that ionizes the molecule via the superexcited state. We note specifically that this experiment does not probe the time dependence of the superexcited state. Rather, it investigates the dependence of the ionization pathway, via the highly excited electronic states, on the internal conversion dynamics between S_2 and S_1. The time-dependent photoelectron spectra are shown as a contour plot in Figure 5. The polarizations of the 4ω and 2ω pulses in this spectrum were parallel; the signal with perpendicular polarizations was too weak for a measurement of its time dependence.

We first note that much of the three-photon signal rises and decays on the time scale of the instrument function, about 230 fs. In the energy range between 9.4 and 10.3 eV the signal decays completely to the baseline. This decay cannot, within our time resolution, be distinguished from the decay of the $4\omega + 2\omega$, two-photon signal reported previously.[21] However, the photoelectron signal from 10.3 to 11.2 eV does not decay completely. Instead there is a component that persists into the picosecond range. A small energy slice of the peak at 10.4 eV, integrated from 10.3 to 10.6 eV and graphed with respect to the delay time, is shown in Figure 6. An exponential fit to the latter part of the curve gives a decay rate for the slow component of $2.8 \times 10^{11} s^{-1}$.

The slow decay component raises several questions: If the peaks are still to be interpreted as arising from Rydberg states,

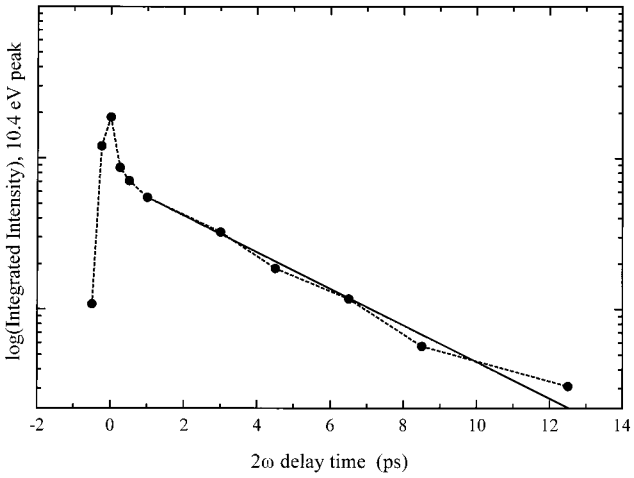

Figure 6. Intensity of the $4\omega + 2\omega + 2\omega$ peak at 10.4 eV as a function of 2ω delay time. The solid curve is a fit to the slow component with a decay rate of 2.8×10^{11} s^{-1}. The laser wavelengths are identical to those in Figure 5.

what mechanism is responsible for their excitation? Why do we see these states for several picoseconds after the S_2 state has decayed? And finally, what causes their decay on a picosecond time scale?

The clue to understand the slowly decaying signal is an observation that we made in the ionization of phenol via the S_1 electronic state, using 3ω and 2ω laser pulses.[22] There we found that the 2ω pulse, with 3 eV photons, can access the Rydberg states from S_1, even though the photon energy is too low to reach the 9 eV superexcited state. It was postulated that this is possible because a transition from orbital 16 to orbital 18 can be induced by the 3 eV second-harmonic photon, leading to a state with an electron configuration of $...(16)^1(17)^2(18)^2(19)^1$. This interpretation is supported by a comparison with photoelectron spectra, as well as absorption spectra of the phenol ion.[29]

We now come to an understanding of the slow component of the $4\omega + 2\omega + 2\omega$ ionization signal. The internal conversion from S_2 populates the S_1 state, which has an electronic energy of 4.5 eV. About 1.5 eV is converted from electronic to vibrational energy. From S_1, the absorption of a 3 eV photon accesses a valence state with an electronic energy of about 7.5 eV. It is likely that much of the vibrational energy remains with the molecule during this second excitation step, so that the molecule is lifted to the 7.5 eV valence state with 1.5 eV of vibrational energy. This highly excited vibronic state rapidly relaxes into those Rydberg states that are energetically available.

Internal conversion from the 9 eV resonance, accessed by the $4\omega + 2\omega$ excitation, can reach all Rydberg states with energies less than 9 eV. This gives rise to photoelectron peaks stretching from 9.5 to 12 eV. When ionizing via the resonance at 7.5 eV, only those Rydberg levels with an electronic energy below 7.5 eV are energetically accessible. For the ionization in the $3\omega + 3\omega + 2\omega$ process, this leads to a sharp onset of the signal above 10.0 eV in the photoelectron spectrum. The time-delayed $4\omega + 2\omega + 2\omega$ spectra in Figure 5 also show an onset of the signal level above 10 eV, even though the onset is not as sudden as in the previously reported spectra. The onset arises from the additional signal that is generated by a pathway to ionization via the S_2 state, internal conversion to S_1, excitation to the 7.5 eV resonance by a 3 eV photon, and subsequent decay to the Rydberg states. At long delay times, after the S_2 state has relaxed, this three-photon ionization via the 7.5 eV resonance dominates over the signal via the 9 eV resonance.

This ionization path via the 7.5 eV resonance is illustrated in the lower part of Figure 4. Upon excitation to S_2, the molecule experiences an internal conversion to S_1, from where it absorbs a 2ω photon to generate a singly excited state with a vacancy in orbital 16. Then, there is a further nonradiative process that populates Rydberg levels with energies below 7.5 eV. The last step is the ionization by another 2ω photon. The oscillator strengths for the transitions from S_1 or S_2 to the highly excited valence states are unknown. On the basis of the fact that the same orbitals are involved, one can surmise that their electronic components are similar. However, given the large amount of vibrational energy after internal conversion to S_1, there could be significant contributions from Franck−Condon overlaps between the involved electronic states. Our experiment is not designed to further explore this point.

The final question to address is the source of the 3.6 ps decay of the three-photon signal stemming from the second pathway. The delay between the 4ω pulse and the 2ω pulse probes the dynamics of the S_1 state populated after internal conversion from S_2. This state, at its origin, is known to have a lifetime of 2 ns,[30] much longer than what we observe. However, upon internal conversion from S_2 to S_1, the molecule has a vibrational energy of 1.5 eV, or about 12000 cm^{-1}. It is possible that the presence of such a large amount of vibrational energy accelerates the electronic relaxation of phenol out of the S_1 state. Such dramatic accelerations have been observed in other molecules.[31−35] Alternatively, it is possible that phenol experiences a proton transfer to form 1,3-cyclohexadien-5-one,[36] on the time scale of our experiment. Since only a hydrogen atom needs to move, this isomerization could proceed on a picosecond time scale. Finally, we point out that a similar decay of the photoelectron signal on a picosecond time scale has been observed by Hayden et al. on 1,3,5-hexatriene.[6,7] They attribute the decay to an IVR process that slowly takes the vibrational energy from the Franck−Condon regime to more outlying areas of the vibrational phase space, leading to a decay of the ionization signal. A similar process could be considered to explain our observations in phenol.

Summary

In addition to the well-known resonance-enhanced two-photon ionization mechanism, our work has revealed several competing resonant pathways that use three photons to ionize the phenol molecule. Upon excitation to either the S_1 or S_2 electronic state, the molecule absorbs an additional photon by populating highly excited valence states. These states relax rapidly into a set of isoenergetic vibronic levels that are well described by the Rydberg formula. Ionization from these levels produces a rich set of photoelectron peaks spanning a wide energy range.

From the S_2 electronic state of phenol, two photons of 3 eV each can ionize the molecule. The ionization likely proceeds via an optically bright superexcited state at 9 eV. Polarization experiments, as well as the orbital transition energies, are consistent with a description of this state as having an electron configuration of $...(16)^1(17)^2(18)^2(19)^0(20)^1$. Our previous work has shown that there is also an admixture of the configuration $...(16)^2(17)^2(18)^0(19)^2(20)^0$. Since both these configurations have A_1 symmetry, it appears likely that we observe a single, highly mixed, superexcited valence state. This state rapidly relaxes into the set of Rydberg states converging to the $\tilde{X}$ ions.

The S_2 state undergoes a rapid nonradiative decay to the S_1 electronic state. After the relaxation, the molecule can again absorb a photon, to generate a highly excited vibronic state at 7.5 eV. On the basis of the known He(I) photoelectron spectrum

of phenol, as well as the absorption spectrum of the phenol ion,[29] we associate this 7.5 eV state with an electron configuration of $...(16)^1(17)^2(18)^2(19)^1$. This valence state is again very short lived, relaxing into the same set of Rydberg states that are populated in the pathway via the superexcited state at 9 eV. However, only those Rydberg states with energies below 7.5 eV are available.

The absorption from S_1 to the 7.5 eV state provides an ionization pathway that persists after the internal conversion from S_2 to S_1. The time-resolved experiments show that the highly vibrationally excited S_1 state has a decay rate of 2.8×10^{11} s^{-1}.

All of our experiments were performed with the titanium: sapphire laser tuned to a photon energy of the fundamental laser output near 1.5 eV. This is convenient since the S_1 transition requires one third-harmonic (3ω) photon while the S_2 transition needs one fourth-harmonic (4ω) photon. The second-harmonic photons, 2ω, were then used to probe the excited states. It may be considered curious that so many ionization pathways are observed with fixed-frequency photons. However, this is probably not entirely accidental. The photons are tuned to molecular resonances that reflect differences in orbital energies. To the extent that the orbital energies do not change upon electronic excitation, a second photon of the same energy can lift the second electron to a higher state as well. Since the resulting highly excited valence states are very short lived, the bands are expected to be broad. The energy matching may therefore be possible in many molecules and could be frequently observed, especially in experiments with femtosecond time resolution. On the other hand, the fact that a 2ω photon, with an energy of just half the S_0-S_2 gap, and 2/3 of the S_0-S_1 gap, can be absorbed to fill the very same HOMO that is vacated by the first transition may well be specific to phenol. Other molecules may feature similar transitions; however, the energies required for such transitions may differ.

Last, we address the relevance of our work to time-resolved measurements of electronic relaxation phenomena with multiphoton ionization techniques in general. As we have seen, there are a bewildering number of processes that can occur at laser intensities that are typical for resonance ionization experiments. In addition to the expected two-photon ionization mechanisms, there are several doubly resonant three-photon ionization pathways. These processes take advantage of the very large number of electronic states that are present in molecules at high electronic energies. Such states include doubly excited valence states, states with vacancies below the HOMO, and Rydberg states. Many experiments have been performed where only the mass of the ion is recorded as a function of delay time between different laser pulses. In analyzing those experiments, one assumes that the desired two-photon ionization process dominates the signal. While this may be true for very small delay times, exceptions may occur at larger delay times where the two-photon signal subsides. At these larger delay times, alternative ionization mechanisms may dominate, leading to double-exponential decays that could be easily misinterpreted.

As far as technique is concerned, it is far preferable to observe time-dependent photoelectron spectra rather than mass spectra. Even so, one has to carefully analyze the spectra to ascertain that the particular process of interest is indeed the one that yields the signal, even at long delay times after the dominant ionization process subsides. Our work has shown that this analysis can be quite challenging, as the number of possible processes is very large. However, such studies are also extremely rewarding because we continue to learn about the complexity of excited-state dynamics in molecules.

Acknowledgment. This research was supported, in part, by funding from the Army Research Office (Grants DAAH04-96-1-0188 and DAAD19-00-1-0141). C.P.S. acknowledges support through a Rhode Island NASA Space Grant Fellowship (Grant NGT5-90014).

References and Notes

(1) Sekreta, E.; Reilly, J. P. *Chem. Phys. Lett.* **1988**, *149*, 482.
(2) Song, X.; Wilkerson, C. W., Jr.; Lucia, J.; Pauls, S.; Reilly, J. P. *Chem. Phys. Lett.* **1990**, *174*, 377.
(3) Hillenbrand, S.; Zhu, L.; Johnson, P. *J. Chem. Phys.* **1990**, *92*, 870.
(4) Hillenbrand, S.; Zhu, L.; Johnson, P. *J. Chem. Phys.* **1991**, *95*, 2237.
(5) Smith, J. M.; Zhang, X.; Knee, J. L. *J. Phys. Chem.* **1995**, *99*, 1768.
(6) Hayden, C. C.; Chandler, D. W. *J. Phys. Chem.* **1995**, *99*, 7897.
(7) Cyr, D. R.; Hayden, C. C. *J. Chem. Phys.* **1996**, *104*, 771.
(8) Radloff, W.; Stert, V.; Freudenberg, T.; Hertel, I. V.; Jouvet, C.; Denonder-Lardeux, C.; Solgadi, D. *Chem. Phys. Lett.* **1997**, *281*, 20.
(9) Fischer, I.; Villeneuve, D. M.; Vrakking, M. J. J.; Stolow, A. *J. Chem. Phys.* **1995**, *102*, 5566.
(10) Blanchet, V.; Zgierski, M. Z.; Seideman, T.; Stolow, A. *Nature* **1999**, *401*, 52.
(11) Zanni, M. T.; Taylor, T. R.; Greenblatt, B. J.; Soep, B.; Neumark, D. M. *J. Chem. Phys.* **1997**, *107*, 7613.
(12) Greenblatt, B. J.; Zanni, M. T.; Neumark, D. M. *Science* **1997**, *276*, 1675.
(13) Greenblatt, B. J.; Zanni, M. T.; Neumark, D. M. *Faraday Discuss.* **1998**, *108*, 101.
(14) Zanni, M. T.; Lehr, L.; Greenblatt, B. J.; Weinkauf, R.; Neumark, D. M. *Ultrafast Phenom. XI, Proc. Int. Conf., 11th, 1998* **1998**, *63*, 474.
(15) Weber, P. M.; Thantu, N. *Chem. Phys. Lett.* **1992**, *197*, 556.
(16) Thantu, N.; Weber, P. M. *Chem. Phys. Lett.* **1993**, *214*, 276.
(17) Thantu, N.; Weber, P. M. *Z. Phys. D: At., Mol. Clusters* **1993**, *28*, 191.
(18) Kim, B.; Thantu, N.; Weber, P. M. *J. Chem. Phys.* **1992**, *97*, 5384.
(19) Kim, B.; Schick, C. P.; Weber, P. M. *J. Chem. Phys.* **1995**, *103*, 6903.
(20) Kim, B.; Weber, P. M. *J. Phys. Chem.* **1995**, *99*, 2583.
(21) Schick, C. P.; Carpenter, S. D.; Weber, P. M. *J. Phys. Chem. A* **1999**, *103*, 10470.
(22) Schick, C. P.; Weber, P. M. *J. Phys. Chem. A* **2001**, *105*, 3725.
(23) Stolow, A. Private communication, 1999.
(24) Thantu, N. Ph.D. Thesis, Brown University, Providence, RI, 1993.
(25) Carpenter, S. D.; Schick, C. P.; Weber, P. M. *Rev. Sci. Instrum.* **1999**, *70*, 2262.
(26) Müller-Dethlefs, K.; Schlag, E. W. *Annu. Rev. Phys. Chem.* **1991**, *42*, 109.
(27) Lipert, R. J.; Colson, S. D. *J. Chem. Phys.* **1990**, *92*, 3240.
(28) Bist, H. D.; Brand, J. C. D.; Williams, D. R. *J. Mol. Spectrosc.* **1996**, *21*, 76.
(29) Kesper, K.; Diehl, F.; Simon, J. G. G.; Specht, H.; Schweig, A. *Chem. Phys.* **1991**, *153*, 511.
(30) Lipert, R. J.; Bermudez, G.; Colson, S. D. *J. Phys. Chem.* **1988**, *92*, 3801.
(31) Sobolewski, A. L. *Chem. Phys.* **1987**, *115*, 469.
(32) Hornburger, H. *Z. Phys. D: At., Mol. Clusters* **1989**, *11*, 129.
(33) Dujardin, G.; Leach, S. *J. Chem. Phys.* **1983**, *79*, 658.
(34) Woudenberg, T. M.; Kulkarni, S. K.; Kenny, J. E. *J. Chem. Phys.* **1988**, *89*, 2789.
(35) Kulkarni, S. K.; Kenny, J. E. *J. Chem. Phys.* **1988**, *89*, 4441.
(36) Russell, D. H.; Gross, M. L.; Nibbering, N. M. M. *J. Am. Chem. Soc.* **1978**, *100*, 6133.